

**MAX-PLANCK-INSTITUT FÜR PLASMAPHYSIK**  
**GARCHING BEI MÜNCHEN**

Integrable and Nonintegrable  
Non-KAM Hamiltonians  
and Magnetic Field Topology

A. Salat

IPP 6/ 257

January 1986

*Die nachstehende Arbeit wurde im Rahmen des Vertrages zwischen dem  
Max-Planck-Institut für Plasmaphysik und der Europäischen Atomgemeinschaft über  
die Zusammenarbeit auf dem Gebiete der Plasmaphysik durchgeführt.*

## Abstract

The integrability of Hamiltonians  $H(P_1, P_2, Q_1, Q_2) = P_1 G_1(Q_1, Q_2) + P_2 G_2(Q_1, Q_2)$ , with arbitrary analytic  $G_1$  and  $G_2$ ,  $2\pi$ -periodic in  $Q_1$  and  $Q_2$ , is analytically investigated. Such  $H$  cannot be separated into two parts,  $H = H_0 + H_1$ , such that the KAM theorem would apply for  $|H_1| \ll |H_0|$ .

For  $G_2 = \text{const}$  such Hamiltonians correspond to toroidal magnetic fields with constant rotational transform. Integrability is then equivalent to the existence of closed magnetic surfaces.

The winding number  $w$  of the  $Q_1, Q_2$  flow (i.e. the rotational transform) is rational in "tongue" -like domains in  $(\omega_2/\omega_1, A)$  diagrams. Here  $\omega_i = \langle G_i \rangle$  is the average over both  $Q_1$  and  $Q_2$ ,  $G_i = \omega_i + F_i$ ,  $i = 1, 2$ , and  $A$  is an amplitude parameter of  $F_i$  ( $F_i = 0$  for  $A = 0$ ). Integrability is proved almost everywhere in the complementary domains, namely where  $w$  is sufficiently irrational.

In the generic case ("conditional") nonintegrability is proved for the class  $\partial G_1/\partial Q_1 + \partial G_2/\partial Q_2 = 0$  in the tongues, which in this case shrink to lines with  $w = \omega_1/\omega_2$ .

It is shown that if the number of dimensions in the Hamiltonian were larger than two, qualitatively different results would be expected.

## 1. Introduction

The equations for magnetic field lines can be written as a one-dimensional, time-dependent or a two-dimensional, time-independent Hamiltonian system with the Hamiltonian

$$H(P_1, P_2, Q_1, Q_2) = h(P_1, Q_1, Q_2) + P_2 G_2, \quad (1.1)$$

where  $Q_1$  and  $Q_2$  are a poloidal and a toroidal angle,  $h$  is  $2\pi$ -periodic in  $Q_1$ ,  $Q_2$ , and  $G_2 = \text{const}$  /1/. Integrability of such Hamiltonians is equivalent to the existence of toroidal magnetic surfaces. Hamiltonians with

$$h = P_1 G_1(Q_1, Q_2) \quad (1.2)$$

correspond to toroidal magnetic fields with constant rotational transform /2/.

Motivated by this connection with field line topology, by general interest in this particular type (see below) of Hamiltonians, and by previous numerical studies /3/ on integrability, we study analytically whether Hamiltonians of the general form

$$H = P_1 G_1(Q_1, Q_2) + P_2 G_2(Q_1, Q_2), \quad (1.3)$$

with  $G_1$  and  $G_2$   $2\pi$ -periodic in  $Q_1$ ,  $Q_2$ , are integrable.

A two-dimensional Hamiltonian is called integrable /4/ if there exists another linearly independent single-valued function  $I(P_1, P_2, Q_1, Q_2)$  which is a constant of the motion and which can be solved for  $P_1$  or  $P_2$ . In this case the equations of motion can be reduced to quadratures, and the Hamiltonian is transformed into  $\hat{H}(\hat{P}_1, \hat{P}_2)$ , which implies motion on nested tori with radii  $\hat{P}_1, \hat{P}_2 = \text{const}$  if the accessible region of phase space is finite.

Usually, periodic Hamiltonians arise from problems where  $Q_1$  and  $Q_2$  either are angles, as in the present case, or are related to physical quantities via periodic canonical

transformations. In these cases single-valuedness of the underlying physics requires that  $I$  also be periodic in  $Q_1, Q_2$  with the same periodicity as  $H$ . It may therefore be useful to distinguish nonintegrable Hamiltonians ( $I$  non-single-valued in  $Q_1, Q_2$ ) from “conditionally nonintegrable” ones ( $I$  single-valued in  $Q_1, Q_2$  but not periodic). With respect to magnetic fields these two cases correspond to nonexistence of magnetic surfaces and to their degeneracy into purely “radial” segments, respectively.

The majority of Hamiltonians seem to be nonintegrable /4/. The theory of Kolmogorov, Arnold and Moser ( KAM ) /5/, however, asserts that a small perturbation  $H_1(P_1, P_2, Q_1, Q_2)$ ,  $H_1$  periodic, of an integrable Hamiltonian  $H_0(P_1, P_2)$ ,  $H = H_0 + H_1$ , preserves a large measure of the unperturbed phase space tori. Potential “chaos” is therefore then confined to the regions between surviving tori, i.e. magnetic surfaces. KAM theory requires /5/ that

$$\det \left\{ \frac{\partial^2 H_0}{\partial P_i \partial P_j} \right\} \neq 0 \quad (1.4)$$

(or a slightly different condition which for the present considerations is equivalent ). Condition (1.4) is violated if  $H_0$  does not contain either  $P_1$  or  $P_2$  (“proper degeneracy”) or if it is linear in  $P_1$  and  $P_2$  (“limiting degeneracy”). In /6/ KAM theory was generalized to include these cases, provided  $H_1$  is nonlinear in  $P_1, P_2$ .

This remedy cannot be applied if the total Hamiltonian is linear in the momenta, as in eq. (1.3). Such Hamiltonians have been termed “non-KAM” and have been preliminarily investigated in /3/. The purpose of the present paper is to elucidate and prove that Hamiltonians (1.3) with analytic  $G_1, G_2$  are integrable in certain parameter domains characterized by irrational winding number (i.e. rotational transform), and that, at least for  $\partial G_1 / \partial Q_1 + \partial G_2 / \partial Q_2 = 0$  and other subclasses, there is an infinity of conditionally nonintegrable cases with rational winding numbers squeezed in between the integrable ones.

In Sec. 2 previous, mostly numerical, results /3/ are briefly recapitulated. The reduction of the canonical equations to two-dimensional "non-KAM" mappings and their properties are discussed in Sec. 3. The main result of the paper, the proof of integrability of analytic Hamiltonians (1.3), using results of Sec. 3, is presented in Sec. 4. A short discussion of the difficulties in generalizing the result to higher dimensions than two is given in Sec. 5.

## 2. Review of numerical results

The canonical equations

$$\dot{Q}_i = G_i(Q_1, Q_2) \quad (2.1)$$

$$\dot{P}_i = -P_1 \frac{\partial G_1}{\partial Q_i} - P_2 \frac{\partial G_2}{\partial Q_i}, \quad (2.2)$$

$i=1, 2$ , were numerically solved for a variety of periodic functions  $G_1, G_2$  in /3/. The results were presented in (flow) diagrams showing  $Q_2(t)$  versus  $Q_1(t)$  along typical orbits, and in Poincaré surface-of-section (sos) diagrams showing  $P_1(Q_2)$  in polar coordinates at  $Q_1 \bmod 2\pi = \text{const}$ . Sos diagrams can best be obtained by using  $Q_2$  or  $Q_1$  as a parameter along the orbit, according to

$$\frac{dQ_1}{dQ_2} = \frac{G_1(Q_1, Q_2)}{G_2(Q_1, Q_2)}, \quad (2.3)$$

$$\frac{dP_1}{dQ_2} = -\frac{1}{G_2} \left[ P_1 \frac{\partial G_1}{\partial Q_1} + P_2 \frac{\partial G_2}{\partial Q_1} \right], \quad (2.4)$$

etc. The existence of an invariant  $I$  other than  $H$  shows up in an sos diagram if the successive crossing points of an orbit form a one-dimensional closed curve (the projection of a torus) instead of a two-dimensional accumulation of points.

It was numerically observed in /3/ that Hamiltonians (1.3) are integrable if a single  $Q_1, Q_2$  orbit covers the periodic square (torus)  $0 \leq Q_1 \leq 2\pi, 0 \leq Q_2 \leq 2\pi$  ergodically ("ergodic flow"). This can be seen here in the sos diagrams of Figs. 1a, 1b and 2a, 2b where the corresponding flow diagrams are typically as in Figs. 3a and 4a.

If the orbit is not ergodic but is attracted to a closed curve (see Fig. 3b) or is periodic from the outset (see Fig. 4b), the sos diagram shows one or more exponentially diverging sequences of points,  $|P_1| \rightarrow \infty$  (see Fig. 1c), or linearly diverging sequences (see Fig. 2c). In these cases integrability is left open. A "chaos" of points as is familiar

from nonlinear Hamiltonians was never observed. For the distribution of ergodic versus nonergodic behaviour in parameter space see Sec. 3.

Figs. 1 and 3 are obtained with

$$\begin{aligned} G_1 &= \omega_1 + A_1 \cos(Q_1 + Q_2) , \\ G_2 &= \omega_2 + A_2 \cos(Q_1 - Q_2) , \end{aligned} \tag{2.5}$$

while Figs. 2 and 4 correspond to

$$\begin{aligned} G_1 &= \omega_1 + A_1 \cos Q_2 , \\ G_2 &= \omega_2 + A_2 \cos Q_1 . \end{aligned} \tag{2.6}$$

They are simple representatives of the many other pairs used in /3/. The main difference between eqs. (2.5) and (2.6) is that the flow has no divergence,

$$\operatorname{div} \dot{Q} = \operatorname{div} G = \frac{\partial G_1}{\partial Q_1} + \frac{\partial G_2}{\partial Q_2} = 0 , \tag{2.7}$$

for equation (2.6), a distinction which will again be manifested below ( $Q = (Q_1, Q_2)$ , etc.).

The initial values of  $Q_1$ ,  $Q_2$  and  $P_1$  in the figures are chosen at random, except that  $|P_1| \leq 1$  from the arbitrary normalization  $P_1^2 + P_2^2 = 1$ . The unit distance is marked at the edge of the sos diagrams.

The fact that the sos diagrams change so much if the parameters  $\omega_i$ ,  $A_i$ ,  $i = 1, 2$ , are varied indicates that the integrals of motion are rather nontrivial functions even for such simple Hamiltonians as with eqs. (2.5), (2.6). This is corroborated in the Appendix.

### 3. Two-dimensional non-KAM maps

Consider a surface of section at, for example, some  $Q_2 \bmod 2\pi = Q_{20} = \text{const}$ . Let the values of  $P_1$  and  $Q_1$  be given there. With a fixed value of the Hamiltonian  $H$ ,  $P_2$  is also determined. From these starting values the canonical equations can be integrated until the surface of section is crossed again, this time with values  $Q'_1, P'_1$  (and  $P'_2$ ). Thus, there is a two-dimensional mapping  $(Q_1, P_1) \rightarrow (Q'_1, P'_1)$  from cut to cut. Analogous mappings of course exist for cuts at  $Q_1 \bmod 2\pi = \text{const}$  and for  $P_2$  as well. We shall therefore omit the indices of  $P$  and  $Q$  when appropriate.

As a consequence of the particular structure of eqs. (2.1), (2.2), the mapping of  $Q$  must be independent of  $P_i$ , and the mappings for  $P_i$  must be linear,  $i = 1, 2$ :

$$P'_1 = \alpha(Q) P_1 + \beta(Q) P_2, \quad (3.1)$$

$$P'_2 = \gamma(Q) P_1 + \delta(Q) P_2.$$

If one of the  $P_i$  is eliminated with  $H = \text{const}$ , the structure of the 2-dimensional mapping is obtained as

$$Q' = F(Q), \bmod 2\pi, \quad (3.2a)$$

$$P' = u(Q) P + v(Q), \quad (3.3)$$

where  $u$  and  $v$  are periodic in  $Q$ . The difference between  $Q'$  and  $Q$  must be a periodic function, so that

$$Q' = Q + f(Q), \bmod 2\pi, \quad (3.2)$$

where  $f(Q)$  is also  $2\pi$ -periodic [7]. The Hamiltonian origin of the orbits implies that the mapping  $(Q, P) \rightarrow (Q', P')$  must be area-preserving, i.e.  $\partial(Q', P')/\partial(Q, P) = 1$ . In consequence,  $u(Q)$  and  $F(Q)$  are related by

$$u(Q) = (dF/dQ)^{-1} = (1 + df/dQ)^{-1}. \quad (3.4)$$



The most prominent feature of the “non-KAM” mapping (3.2)-(3.4) is the independence of the  $Q$ -mapping from the  $P$ -mapping. It has this feature in common with, for example, the Kaplan-Yorke-mapping, studied in /8/:

$$Q' = 2 Q, \text{ mod } 2\pi , \quad (3.5)$$

$$P' = u P + \cos(2Q) , \quad (3.6)$$

which for  $u = 0.5$  is also area-preserving. Other 2-dimensional area-preserving maps, such as the radial twist mapping /9/

$$P' = P + v(Q) , \quad (3.7)$$

$$Q' = Q + a(P'), \text{ mod } 2\pi ,$$

which includes the standard mapping /10/, and others /9/, /11/, /12/ have been thoroughly investigated. In all of them “chaos” was observed, together with period-doubling and universal scaling behaviour.

There is a fundamental difference, however, between those mappings and the map (3.2)-(3.4): Either the  $Q$ -iteration is not independent of the  $P$ -iteration or, if it is, the mapping  $Q' \rightarrow Q$  is noninvertible (see eq. (3.5)). In contrast, the iteration (3.2) is always invertible since it originates from a reversible Hamiltonian motion (excluding the case  $G_1 = G_2 = 0$  simultaneously). In consequence, eq. (3.2) alone cannot produce “chaos” and period-doubling behaviour, because in 1-dimensional maps these effects are tied to noninvertibility /9/. Other universal features concerning the transition from torus motion to chaos, based on circle maps of the type (3.2), have been investigated in, for example /13/-/15/. The universal features are observed in the limit where the mapping (3.2) just loses its invertibility. Again, this case is not relevant here.

It is very useful, however, for the subsequent purpose to know the general properties of invertible circle maps (3.2) which were elucidated by, in particular, Denjoy /16/, Herman /17/ and Arnold /7/ (see /7/ for an overview). For discussion purposes the definition of

a winding number is important. The winding number  $w$ , a kind of average slope, of a flow on a 2-dimensional torus surface such as described by eq. (2.3) is defined as

$$w = \lim_{Q_2 \rightarrow \infty} \frac{Q_1(Q_2)}{Q_2} \quad (3.8)$$

and is independent of the arbitrary starting point. (Alternatively, by switching the roles of  $Q_1$  and  $Q_2$  a conjugate winding number is defined.) With a surface-of-section cut the winding number may be carried over to the circle maps (3.2a), (3.2) on the cut:

$$w = \lim_{n \rightarrow \infty} \frac{F^n(Q) - Q}{2\pi n}, \quad (3.9)$$

where  $F^n$  stands for  $F(F(..F(Q)..))$ ,  $n$  times. Also, let

$$f(Q) = 2\pi \Omega + a(Q), \quad \langle a \rangle = 0, \quad (3.10)$$

where  $\langle a \rangle$  is the mean value of  $a(Q)$ .

The winding number  $w$  is a monotonic and continuously increasing function of  $\Omega$ . For  $a(Q)$  not identically zero, however,  $w$  exhibits plateaus at every rational value of  $w$ , so that  $w(\Omega)$  is a stair-like function. At irrational values of  $w$  there is no plateau.  $w$  is rational if and only if there is a fixed point after a finite number of applications of the mapping. With increasing amplitude  $A_a = \max |a(Q)|$ , the rational plateaus of  $w$  become more and more extended, so that in a  $(\Omega, A_a)$  diagram the regions of rational  $w = m/n$  assume a tongue-like shape ("Arnold tongues"). The same shape is obtained in Fig. 5, where some of the tongues,  $w = 1/1, 2/3, 1/2$  and  $1/3$ , are shown as hatched regions in a frequency-amplitude diagram, for a simple but typical Hamiltonian (eq. (2.5)). The coordinates are  $\omega_2$  and  $A = A_1 = A_2$ . The exponential growth of  $|P_1|, |P_2|$ , mentioned in Sec. 2, occurs if the parameters in  $G_1, G_2$  happen to put  $H$  into such a tongue. For Hamiltonians with  $\text{div } \mathbf{G} = 0$ , such as eq. (2.6), the tongues are reduced to the lines  $\omega_2 = m/n, m$  and  $n$  integer, as is easily seen analytically. In this case  $P_1$  and  $P_2$  grow linearly along the orbit.

If  $|A_i|$  are small,  $|A_i/\omega_i| \ll 1$ ,  $i = 1, 2$ , a randomly chosen set of parameters in  $G_1, G_2$  yields an irrational  $w$  and an ergodic flow (Figs. 3 and 4) with great probability.

Herman /17/ has shown that for almost all irrational winding numbers and  $f(Q)$  analytic there exists an analytic transformation of the angle,  $Q = h(q)$ , with  $h(q + 2\pi) = h(q) + 2\pi$ , such that in the new variable  $q$  the circle mapping (3.2) is a rigid rotation. For the excluded set of irrational  $w$ , having Lebesgue measure zero, the inequalities

$$\left|w - \frac{m}{n}\right| \geq \frac{K}{|n|^{2+\tau}} \quad (3.11)$$

are violated for arbitrary  $K, \tau > 0$  for at least one pair of  $(m, n \neq 0)$ . For these "almost rational" numbers the function  $h$  need not be differentiable. The condition of analyticity of the mapping (3.2) is satisfied here if  $G_1$  and  $G_2$  are analytic, which we shall assume in the following.

With Herman's theorem it is already possible to prove integrability of certain classes of Hamiltonians, e.g. those with  $\text{div } \mathbf{G} = 0$ . Instead, we shall use it in a wider context in the next section for all analytic non-KAM Hamiltonians.

Let us return to the full 2-dimensional non-KAM map (3.2)-(3.4). One can chose an arbitrary pair of functions  $f(Q), v(q)$  such as for example

$$\begin{aligned} f(Q) &= 2\pi\Omega + A_1 \sin Q, \\ v(Q) &= c + A_2 \sin(mQ + B_2). \end{aligned} \quad (3.12)$$

For  $m = 2$ ,  $c = 0$  and arbitrary  $A_1, A_2, B_2$ , numerically obtained  $P(Q)$  diagrams from repeated applications of the map indeed show an "integrable" behaviour (a closed curve) for irrational winding numbers (see Fig. 6), and an exponential growth of  $|P|$  for rational  $w$ , exactly as with continuous Hamiltonians. In the more generic case, however, when  $f$  and  $v$  also contain (among other harmonics) the same harmonic of  $Q$ , as in eqs. (3.12) for  $m = 1$ , the typical behaviour of the mapping is a spiral with essentially linear growth,

if the value of  $c$  is not carefully adjusted (see Figs. 7a and 7b). A spiral has not been seen in sos maps of Hamiltonians (1.3). This indicates that not every non-KAM map has a continuous Hamiltonian counterpart. Since maps are so much easier to handle than differential equations, one is always tempted to work with maps. The example, however, shows that caution is advised in order to avoid erroneous conclusions on the original system of equations.

#### 4. Proof of integrability

A canonical transformation of variables will be applied, such that the flow lines in the transformed  $Q_1, Q_2$  plane become straight. This permits analytic discussion of integrability.

The flow in the  $Q_1, Q_2$  plane may be, for example, ergodic, as in Figs. 3a and 4a, covering the plane from one starting point, or the flow lines may all be closed, like the orbit in Fig. 4b, in which case infinitely many starting points are required in order to reach every point on the plane. Let the flow lines, i.e. the solutions of eq. (2.3) be  $R(Q_1, Q_2) = \text{const.}$  Periodicity and uniqueness of the flow require that  $R$  be of the form

$$R(Q_1, Q_2) = a Q_1 - b Q_2 + r(Q_1, Q_2), \quad (4.1)$$

where  $a$  and  $b$  are constants and  $r$  is  $2\pi$ -periodic in both arguments. A canonical transformation is made from  $P_1, P_2, Q_1, Q_2$  to  $p_1, p_2, q_1, q_2$ , namely

$$q_i = \frac{\partial S(p_1, p_2, Q_1, Q_2)}{\partial p_i}, \quad P_i = \frac{\partial S(p_1, p_2, Q_1, Q_2)}{\partial Q_i}, \quad (4.2)$$

$i = 1, 2$ , with the generating function

$$S = p_1 \cdot \left[ Q_1 + \frac{1}{a} r(Q_1, Q_2) \right] + p_2 Q_2. \quad (4.3)$$

This yields

$$\begin{aligned} q_1 &= Q_1 + \frac{1}{a} r(Q_1, Q_2), \\ q_2 &= Q_2 \end{aligned} \quad (4.4)$$

and

$$\begin{aligned} P_1 &= p_1 \cdot \left[ 1 + \frac{1}{a} \frac{\partial r}{\partial Q_1} \right], \\ P_2 &= p_1 \frac{1}{a} \frac{\partial r}{\partial Q_2} + p_2. \end{aligned} \quad (4.5)$$

The Hamiltonian (1.3) becomes

$$H = p_1 G_1 + p_2 G_2 + \frac{1}{a} p_1 \mathbf{G} \cdot \nabla r . \quad (4.6)$$

From  $\dot{Q} \cdot \nabla R = \mathbf{G} \cdot \nabla R = 0$ , by definition of  $R$ , and eq. (4.1) there finally results

$$H(p_1, p_2, q_1, q_2) = \frac{1}{a} (b p_1 + a p_2) G_2(Q_1(q_1, q_2), Q_2(q_1, q_2)) . \quad (4.7)$$

With eqs. (4.4) the flow lines become

$$R = a q_1 - b q_2 = \text{const} , \quad (4.8)$$

which shows that in the new coordinates they are straight. If a cut is made at some arbitrary  $q_2 \bmod 2\pi = \text{const}$  the map  $q_1 \rightarrow q'_1$  around the torus (see Sec. 3) obviously is then a rigid rotation. This implies that eqs. (4.4) can be interpreted as a collection of transformations  $Q_1 = h(q_1)$ , depending on  $Q_2$ , which transform all the possible circle maps (3.2) on the torus to rigid rotation simultaneously.

Equation (4.8) also follows from the first pair (eqs. (4.9)), of Hamilton's equations:

$$\dot{q}_1 = \frac{b}{a} G_2 , \quad \dot{q}_2 = G_2 , \quad (4.9)$$

$$\dot{p}_1 = - \frac{1}{a} (b p_1 + a p_2) \frac{\partial G_2}{\partial q_1} , \quad (4.10)$$

$$\dot{p}_2 = - \frac{1}{a} (b p_1 + a p_2) \frac{\partial G_2}{\partial q_2} . \quad (4.11)$$

Taking  $q_2$  as a variable along the orbit, for example, and, with the numerical value  $H = H_0 = \text{const}$ , one obtains

$$\frac{dp_1}{dq_2} = - H_0 \frac{1}{G_2^2} \frac{\partial G_2}{\partial q_1} = H_0 \frac{\partial}{\partial q_1} \frac{1}{G_2} . \quad (4.12)$$

According to eq. (4.8)

$$q_1 = w q_2 + c , \quad (4.13)$$

where  $c$  is a constant and  $w = b/a$  is the winding number of the maps  $q_1 \rightarrow q'_1$  and  $Q_1 \rightarrow Q'_1$ . The momentum  $p_1$  becomes

$$p_1(q_2) = H_0 \int^{q_2} dq'_2 \frac{\partial}{\partial(wq'_2)} \frac{1}{G_2(Q_1(wq'_2 + c, q'_2), q'_2)}. \quad (4.14)$$

The integrand, say  $J(q'_2, wq'_2)$ , is a quasiperiodic function of  $q'_2$ , i.e. it is  $2\pi$ -periodic in both  $q'_2$  and  $wq'_2$ . The periodicity in  $q'_2$  is obvious, while periodicity in  $wq'_2$  follows from eqs. (4.4), (4.13) because  $Q_1 \rightarrow Q_1 + 2\pi$  for  $q_1 \rightarrow q_1 + 2\pi$  at arbitrary  $Q_2 = q_2$ .

If the integral (4.14) of the quasiperiodic integrand is again a quasiperiodic function (of  $q_2$  and  $wq_2$ ), integrability is proved: According to eqs. (4.4), (4.13)  $p_1$  would then be  $2\pi$ -periodic in both  $Q_1$  and  $Q_2$  and, with eq. (4.5), the following  $2\pi$ -periodic invariant  $I_1$  would be obtained:

$$I_1(P_1, P_2, Q_1, Q_2) = P_1 \cdot \left[ \left( a + \frac{\partial r}{\partial Q_1} \right) \int^{q_2(Q_1, Q_2)} dq' J(q', wq') \right]^{-1}. \quad (4.15)$$

If, on the other hand, the integral (4.14) is not quasiperiodic, the invariant (4.15) is not ( $2\pi$ -) periodic in  $Q_1, Q_2$ , and the Hamiltonian in question is ("conditionally") nonintegrable.

Let us first consider Hamiltonians with parameters such that the flow in the periodic  $Q_1, Q_2$  plane is ergodic with sufficiently irrational winding numbers  $w$  such that the inequalities (3.11) are satisfied for some  $K, \tau > 0$  for all  $m, n \neq 0$ . These are of course cases outside the rational Arnold tongues. According to the theorems mentioned in Sec. 3 the transformation  $Q = h(q)$  of any map  $Q \rightarrow Q'$  on the  $Q$  plane to rigid rotation is then analytic, and hence the collection of transformations, eqs. (4.4), also. The whole integrand  $J$  in eq. (4.14) is therefore analytic. In addition, owing to the derivative  $\partial/\partial(wq'_2)$ , it does not contain a constant term, if one imagines  $J(q, wq)$  expanded into a double Fourier series in  $q$  and  $wq$ . Moser /18/ has proved that under these conditions the integral is indeed an analytic quasiperiodic function of  $q_2$  and  $wq_2$ . This completes the proof of integrability.

In the Appendix explicit doubly infinite Fourier series representations of the invariant  $I_1$  (rather of a combination  $I$  of  $I_1$  and  $H$ ) are derived for a typical Hamiltonian by expanding in  $|A_i| \ll 1$ . The series are found to be “adelphic” /19/.

Let us then consider ergodic flows with “almost rational”, irrational winding numbers, such that the inequalities (3.11) are not satisfied for some  $m$ ,  $n \neq 0$ . In these pathological cases, according to Sec. 3 the transformation to rigid rotation need not be differentiable any more. In consequence, the canonical transformations (4.5) need not exist since they contain derivatives of  $r(Q_1, Q_2)$ . Thus, the behaviour on the boundaries between the ergodic regions and the rational Arnold tongues may be pathological. This is paralleled by difficulties in the numerical solution of the canonical equations: the elongation of the closed surface-of-section diagrams tends to infinity in approaching these boundaries.

Inside the regions (tongues) with rational winding numbers different field lines come infinitely close together in general (in Fig. 3b a second field line would end up in the same attractor). Hence,  $\partial R/\partial Q_i$  again tends to infinity. Integrability inside the tongues therefore also remains undecided in the general case. There exist Hamiltonians ( $H = P_1 G_1(Q_1) + P_2 G_2(Q_2)$ , for example) which are trivially integrable even for rational winding numbers ( $I_1 = P_1 G_1$ ), but they are most probably not generic.

Finally, let us consider the special case of Hamiltonians with rational winding numbers  $w = m/n$  and all field lines closed, e.g. the class with  $\text{div } \mathbf{G} = 0$  and  $\omega_1/\omega_2 = m/n$ . (Another, but more degenerate, class would be  $G_1 = mG_2/n$ , with  $\text{div } \mathbf{G} \neq 0$ .) In this case  $\partial R/\partial Q_i$  remains finite.  $Q_1(Q_2)$ , and hence the integrand in eq. (4.14), is periodic in  $q_2'$  with period  $2\pi n$ . In the generic case its average, say  $J_0$ , does not vanish, so that the integral has a secular contribution  $\sim J_0 \cdot q_2$ . With each full revolution of  $q_2$ , according to eq. (4.13),  $q_1$  changes by  $2\pi m/n$ , and  $p_1$  grows by a fixed amount. After  $n$  revolutions  $q_1$  (and  $Q_1$ ) returns to its initial value. This implies that the surface-of-section cuts show  $n$



sequences of points growing linearly in the radial direction, in conformity with numerical results (see Fig. 2c). This behaviour proves that no single-valued  $2\pi$ -periodic invariant exists, a situation called “conditional nonintegrability” in Sec. 1.

## 5. Discussion

Analytic Hamiltonians (1.3) have been proved to be integrable in domains where the flow  $Q_1(t), Q_2(t)$  is sufficiently ergodic on the torus  $0 \leq Q_1, Q_2 \leq 2\pi$ . The proof is based on the powerful tool provided by theorems of Denjoy /16/ and Herman /17/ which imply, crudely speaking, the equivalence of ergodic motion on a two-dimensional torus surface with a rigid helical rotation around the torus.

If the number of dimensions is larger than two, no analogous theorems exist. In fact, for  $\mathbf{Q} = (Q_1, Q_2, \dots, Q_n)$ ,  $n = 4$ , for example, the canonical equations (2.1) for  $Q_i$ ,  $i = 1, \dots, 4$  may themselves be a two-dimensional Hamiltonian system: for

$$\frac{\partial G_1}{\partial Q_1} + \frac{\partial G_2}{\partial Q_2} = 0 \quad \text{and} \quad \frac{\partial G_3}{\partial Q_3} + \frac{\partial G_4}{\partial Q_4} = 0, \quad (5.1)$$

for example, all conditions are satisfied to interpret eqs. (2.1) as canonical equations from a Hamiltonian  $\tilde{H}(\tilde{P}_1, \tilde{P}_3, Q_1, Q_3)$  with  $\tilde{P}_1 = Q_2$ ,  $\tilde{P}_3 = Q_4$ . Such nonlinear (in  $\tilde{P}_1, \tilde{P}_3$ ) Hamiltonians, however, are known to exhibit chaotic behaviour in general. The flow of  $(Q_1, Q_2, Q_3, Q_4)$  may thus be totally different from the case  $n = 2$ . What this implies for the integrability of Hamiltonians (1.3) remains to be clarified for  $n \geq 3$ .

## Appendix

If the Hamiltonian (1.3) is integrable according to Sec. 4, it must have an invariant of the form

$$I(P_1, P_2, Q_1, Q_2) = P_1 \sigma(Q_1, Q_2) + P_2 \tau(Q_1, Q_2), \quad (\text{A.1})$$

where  $\sigma$  and  $\tau$  are  $2\pi$ -periodic in  $Q_1$  and  $Q_2$ . The condition  $\dot{I} = [I, H] = 0$  yields

$$P_1 A(Q_1, Q_2) + P_2 B(Q_1, Q_2) = 0 \quad (\text{A.2})$$

with

$$\begin{aligned} A &= G_1 \frac{\partial \sigma}{\partial Q_1} + G_2 \frac{\partial \sigma}{\partial Q_2} - \sigma \frac{\partial G_1}{\partial Q_1} - \rho \frac{\partial G_1}{\partial Q_2}, \\ B &= G_1 \frac{\partial \rho}{\partial Q_1} + G_2 \frac{\partial \rho}{\partial Q_2} - \sigma \frac{\partial G_2}{\partial Q_1} - \rho \frac{\partial G_2}{\partial Q_2}. \end{aligned} \quad (\text{A.3})$$

For a solution  $P_1, P_2$  of eqs. (1.3), (A.1) and (A.2) to exist, with  $I$  linearly independent of  $H$ , one obtains the relations

$$\begin{aligned} A &= B = 0, \\ \rho G_1 - \sigma G_2 &\neq 0. \end{aligned} \quad (\text{A.4})$$

Let the Fourier representation of  $\sigma$  and  $\tau$  be given by

$$\sigma(Q_1, Q_2) = \sum_{m,n=-\infty}^{+\infty} \sigma_{m,n} e^{i(mQ_1+nQ_2)} \quad (\text{A.5})$$

etc. In the following, for definiteness we restrict the discussion to a simple model Hamiltonian: eq. (2.5). From eq. (A.4) one obtains the recursions

$$\begin{aligned}
2 \sigma_{m,n} \Omega_{m,n} = & - A_1 [(m-2)\sigma_{m-1,n-1} + (m+2)\sigma_{m+1,n+1}] \\
& - A_2 [(n+1)\sigma_{m-1,n+1} + (n-1)\sigma_{m+1,n-1}] \\
& + A_1 [\rho_{m-1,n-1} - \rho_{m+1,n+1}]
\end{aligned} \tag{A.6}$$

$$\begin{aligned}
2 \rho_{m,n} \Omega_{m,n} = & - A_1 [(m-1)\rho_{m-1,n-1} + (m+1)\rho_{m+1,n+1}] \\
& - A_2 [(n+2)\rho_{m-1,n+1} + (n-2)\rho_{m+1,n-1}] \\
& + A_2 [\sigma_{m-1,n+1} - \sigma_{m+1,n-1}]
\end{aligned} \tag{A.7}$$

with

$$\Omega_{m,n} = m \omega_1 + n \omega_2 . \tag{A.8}$$

For  $A_1, A_2 = O(\epsilon)$ ,  $\epsilon \ll 1$ , eqs. (A.6), (A.7) yield  $\sigma^k, \rho^k$  from  $\sigma^{k-1}, \rho^{k-1}$ , with

$$\sigma = \sigma^0 + \epsilon \sigma^1 + \epsilon^2 \sigma^2 + \dots \tag{A.9}$$

For  $\omega_2/\omega_1$  irrational, all  $\Omega_{m,n}$  except  $\Omega_{0,0}$  are different from zero. Starting from arbitrary  $\rho_{0,0}^0, \sigma_{0,0}^0$ , with  $\rho_{0,0}^0 \omega_1 \neq \sigma_{0,0}^0 \omega_2$ , one obtains the invariant  $I$ , the number of Fourier modes in each order  $k \geq 0$  growing with  $k$ . When the recursions (A.6), (A.7) are numerically evaluated, and a surface-of-section diagram is analytically determined from  $I, H = \text{const}$ , one obtains excellent agreement with a numerical solution of the orbits (see Fig. 8). The dots correspond to the numerical solution, and the curve is obtained from the analytic representation of the invariant,  $k = 9$  orders being used in the expansion. The series for  $\sigma$  and  $\rho$  are semiconvergent, however, because the agreement is lost if  $k$  is increased too much. Also, there are critical amplitudes  $|A_1|, |A_2|$ , depending on  $\omega_2$ , above which the series no longer converge for arbitrarily high  $k$ .

For  $\omega_2/\omega_1$  rational, the recursions (A.6), (A.7) are much more difficult to handle. For  $\omega_2/\omega_1 = 0.5$ , for example, the left-hand sides vanish for all  $n = -2m, m = 0, \pm 1$ ,

$\pm 2, \dots$ . This yields extra conditions on the right-hand sides. As a result the resonant terms  $\sigma_{m,-2m}^k, \rho_{m,-2m}^k$  are only determined implicitly at orders  $k+2, k+4$ , etc. Starting again with arbitrary  $\sigma_{0,0}^0 \neq 2\rho_{0,0}^0$ , one thus obtains at, for example, order 2 the extra terms

$$\sigma_{2,-4}^2 = \rho_{2,-4}^2 = \frac{3A_1 A_2^3}{2\omega_1^2 (A_1^2 + 2A_2^2)} (\sigma_{0,0}^0 - 2\rho_{0,0}^0). \quad (\text{A.10})$$

The agreement between the analytic and the numerical solution is again good, see Fig. 9, which was obtained for  $k = 4$ . (This low number of iterations restricts one to mild deviations from the trivial case  $P_1 = \text{const}$  at  $A_1 = A_2 = 0$ ).

Integrals of the motion with the typical properties of the two series discussed above (“adelphic” integrals) were studied in /19/ for nonlinear Hamiltonians.

## Acknowledgement

The author would like to thank B. Chirikov<sup>1</sup>, H. Wimmel and G. Spies for helpful discussions.

---

<sup>1</sup>Institute of Nuclear Physics, Novosibirsk, USSR

## Figure captions

Fig. 1a: Surface-of-section values  $P_1(Q_1)$  at  $Q_2 \bmod 2\pi = \text{const}$ , case (2.5);  $A_1 = A_2 = 0.2$ ;  $\omega_1 = 1.0$  throughout,  $\omega_2 = 0.521111$ ;  $N = 1000$  revolutions around the torus.

Fig. 1b:  $P_1(Q_1)$ , case (2.5);  $A_1 = A_2 = 0.3$ ;  $\omega_2 = 0.531$ ;  $N = 1000$ .

Fig. 1c:  $P_1(Q_1)$ , case (2.5);  $A_1 = A_2 = 0.1$ ;  $\omega_2 = 0.898$ ;  $N = 155$ .

Fig. 2a:  $P_1(Q_1)$ , case (2.6);  $A_1 = A_2 = 0.3$ ;  $\omega_2 = 0.521111$ ;  $N = 1000$ .

Fig. 2b:  $P_1(Q_2)$ , case (2.6);  $A_1 = A_2 = 0.8$ ;  $\omega_2 = 0.521111$ ;  $N = 2400$ .

Fig. 2c:  $P_1(Q_2)$ , case (2.6);  $A_1 = A_2 = 0.1$ ;  $\omega_2 = 0.5$ ;  $N = 100$ .

Fig. 3a: Ergodic orbit  $Q_2(Q_1)$ , case (2.5);  $A_1 = A_2 = 0.2$ ;  $\omega_2 = 0.521111$ .

Fig. 3b: Attracted orbit  $Q_2(Q_1)$ , case (2.5);  $A_1 = A_2 = 0.1$ ;  $\omega_2 = 0.898$ .

Fig. 4a: Ergodic orbit  $Q_2(Q_1)$ , case (2.6);  $A_1 = A_2 = 0.3$ ;  $\omega_2 = 0.521111$ .

Fig. 4b: Periodic orbit  $Q_2(Q_1)$ , case (2.6);  $A_1 = A_2 = 0.1$ ;  $\omega_2 = 0.5$ .

Fig. 5 : Some regions (hatched) of rational winding numbers  $w$ , case (2.5);  $A = A_1 = A_2$ .

Fig. 6 : Iterates of non-KAM map (3.2) - (3.4) in polar coordinates, case (3.11);  $m = 2, c = 0$ ;  $A_1 = 0.4, A_2 = 0.8$ ;  $\Omega = 0.521111$ ;  $N = 1000$ .

Fig. 7a: Non-KAM map, case (3.12);  $m = 2, c = 0$ ;  $A_1 = A_2 = 0.2$ ;  $\Omega = 0.521111$ ;  $N = 800$ .

Fig. 7b: Same as Fig. 7a, but with  $c = 0.01977$ ;  $N = 800$ .

Fig. 8 : Comparison of  $P_1(Q_2)$ , case (2.5), from numerical solution (dots) and analytic invariant (curve);  $A_1 = A_2 = 0.12$ ;  $\omega_2 = 0.851111$ ;  $N = 200$ .

Fig. 9 : Comparison for rational  $\omega_2/\omega_1 = 0.5$ ,  $A_1 = A_2 = 0.12$ ;  $N = 200$ .

## References

- /1/ K.J. Whiteman, Rep. Prog. Phys. 40 (1977) 1033.
- /2/ A. Salat, Z. Naturforsch. 40a (1985) 959.
- /3/ A. Salat, Z. Naturforsch. 39a (1984) 830.
- /4/ V.I. Arnold and A. Avez, Ergodic Problems of Classical Mechanics, W. Benjamin, Hunter, N.Y. 1968.
- /5/ V.I. Arnold , Russian Math. Surveys 18 (1963) 9.
- /6/ V.I. Arnold , Russian Math. Surveys 18 (1963) 85.
- /7/ V.I. Arnold , Geometrical Methods in the Theory of Ordinary Differential Equations, Springer, New York 1983.
- /8/ D.A. Russel, J.D. Hanson and E. Ott, Phys. Rev. Lett. 45 (1980) 1175.
- /9/ A.J. Lichtenberg and M.A. Lieberman, Regular and Stochastic Motion, Springer, New York 1983.
- /10/ B.V. Chirikov, Phys. Reports 52 (1979) 265.
- /11/ J.M. Greene, R.S. MacKay, F. Vivaldi and M.J. Feigenbaum, Physica 3D (1981) 468.
- /12/ R.H.G. Helleman, in Long-Time Prediction in Dynamics, C. Horton, L. Reichl, V. Szebehely (eds.), Wiley, New York 1983.
- /13/ P. Couillet, C. Tresser and A. Arneodo, Phys. Letters 77A (1980) 327.
- /14/ S.J. Shenker, Physica 5D (1982) 405
- /15/ P. Cvitanović, M.H. Jensen, L.P. Kadanoff and I. Procaccia, Phys. Rev. Lett. 55 (1985) 343.



/16/ A. Denjoy, C. R. Acad. Sci. 195 (1932) 478.

/17/ M.R. Herman, Lecture Notes in Mathematics, Vol. 597, Springer, Berlin 1977.

/18/ J. Moser, SIAM Review 8 (1966) 145.

/19/ E.T. Whittaker, A Treatise on Analytical Dynamics, Cambridge University Press,  
Cambridge 1964.

Fig. 1a

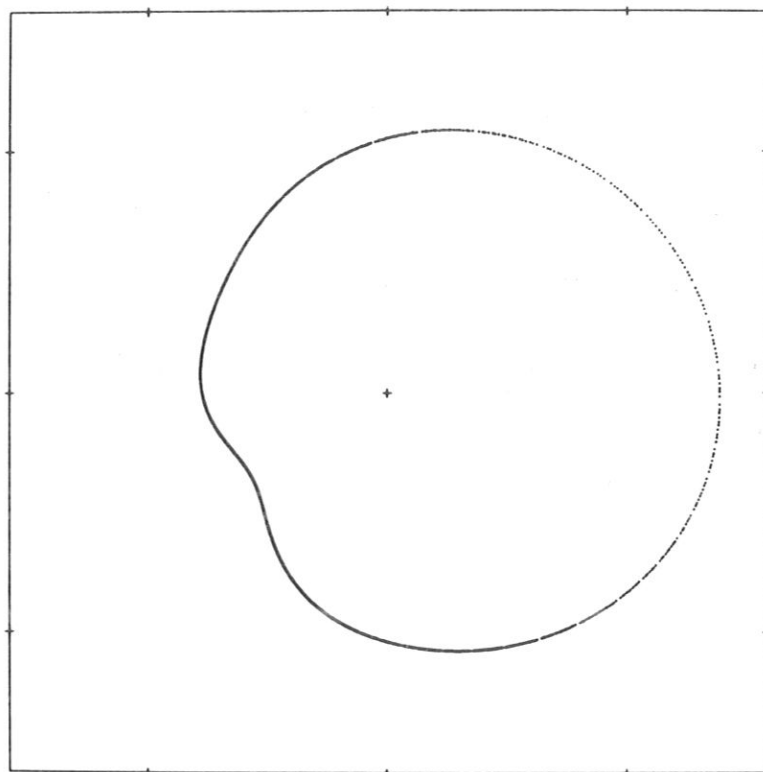


Fig. 1b

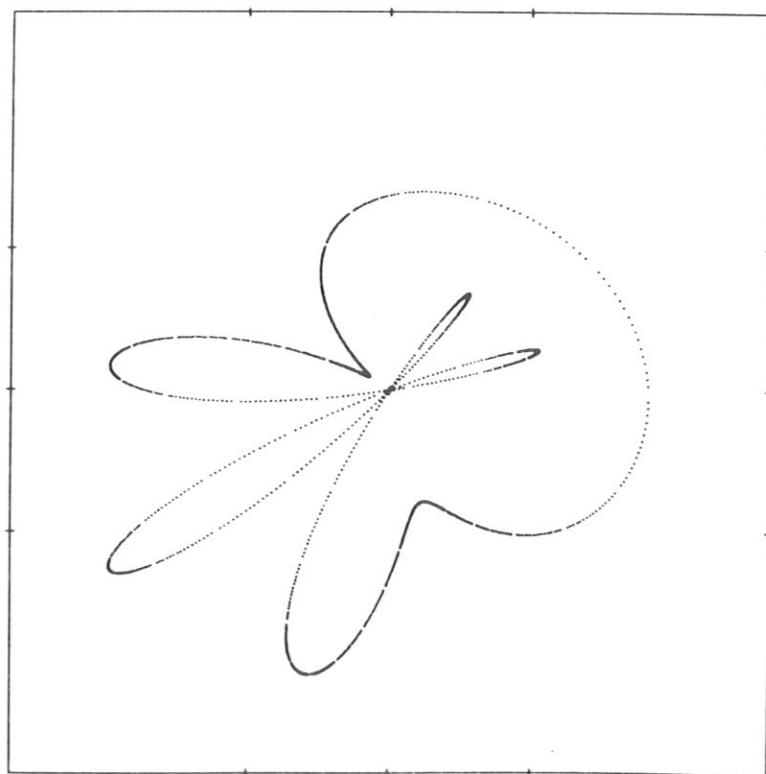


Fig. 1c

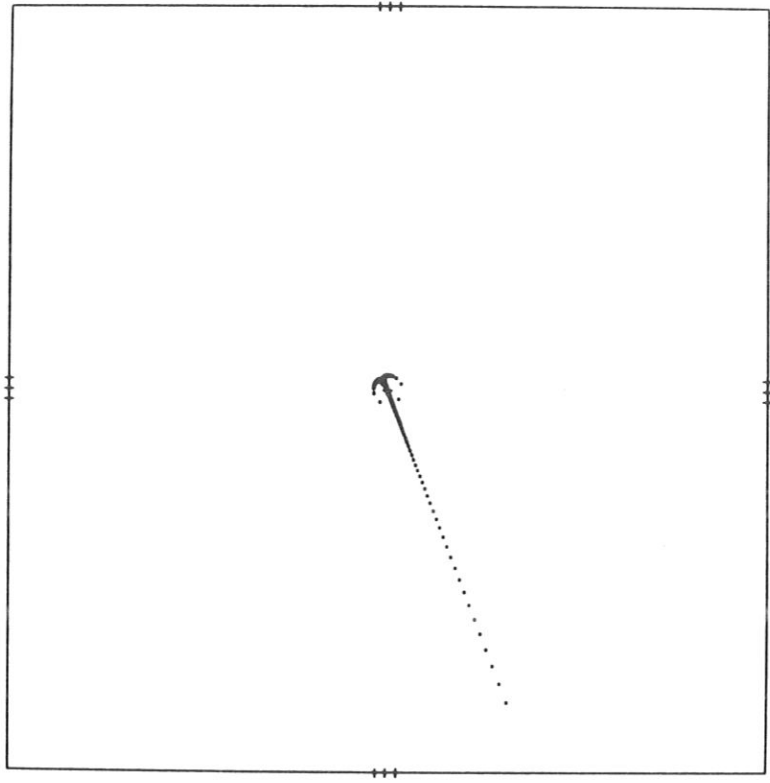


Fig. 2a

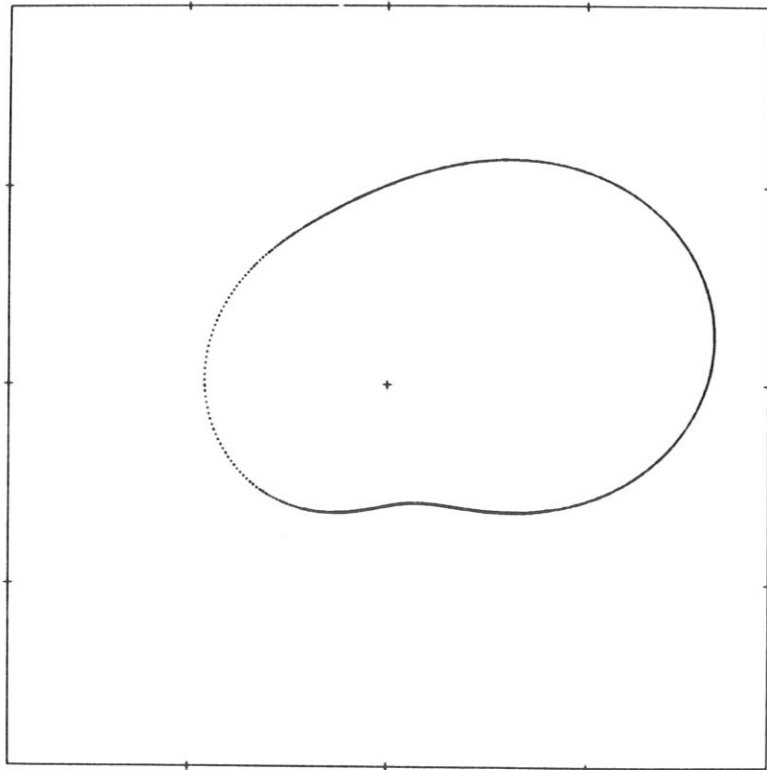


Fig. 2b

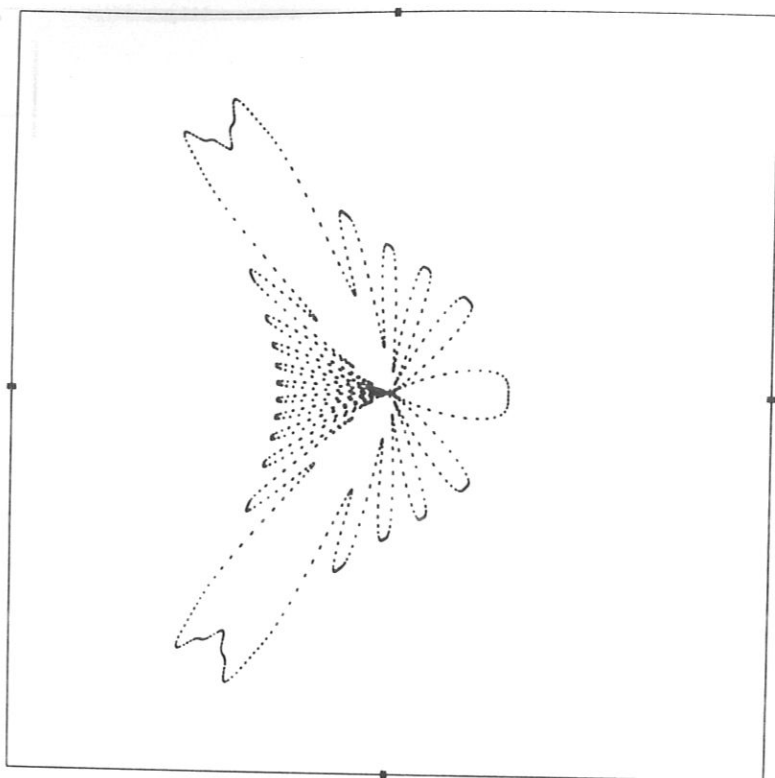


Fig. 2c

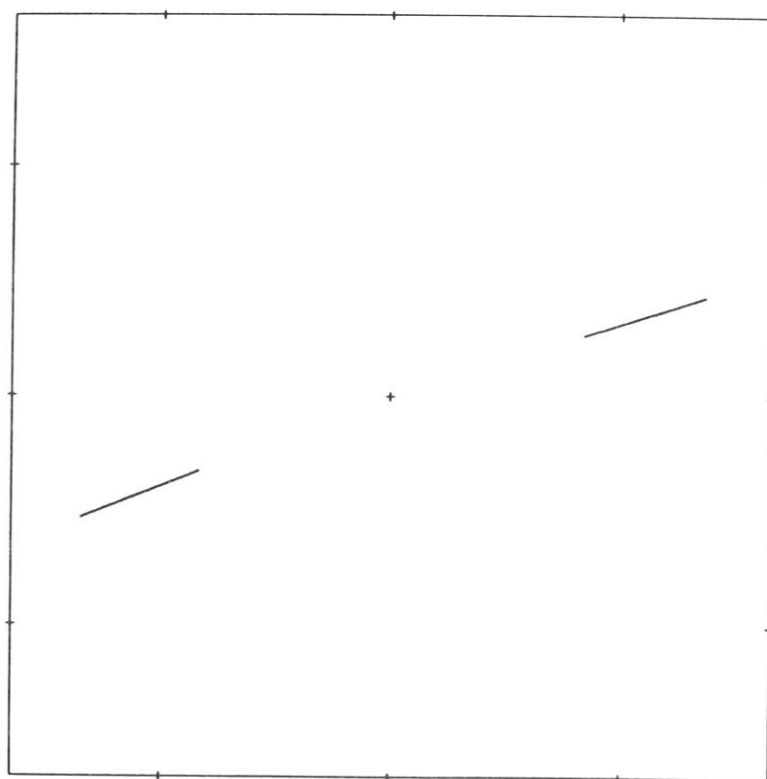


Fig. 3a

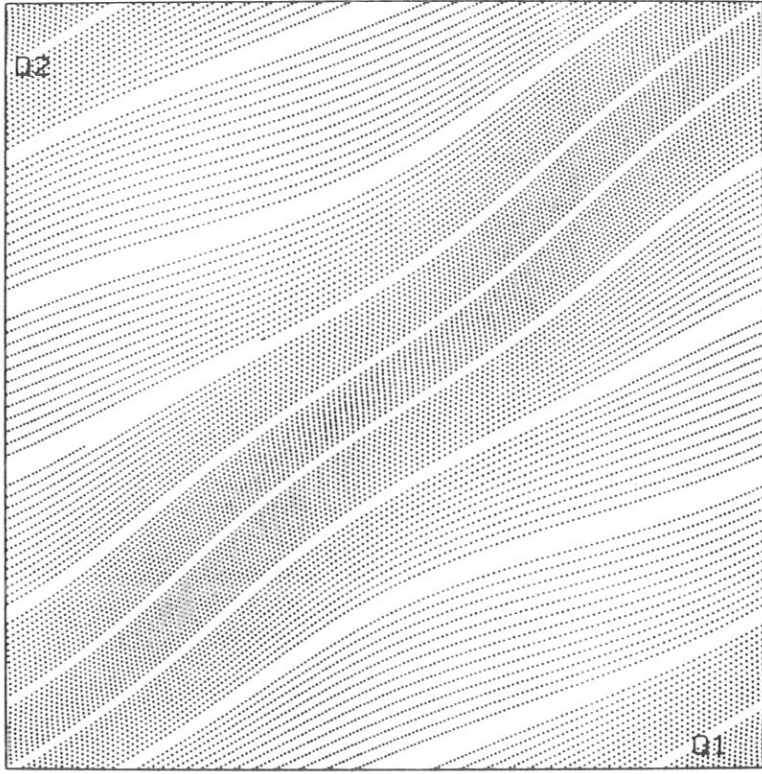


Fig. 3b

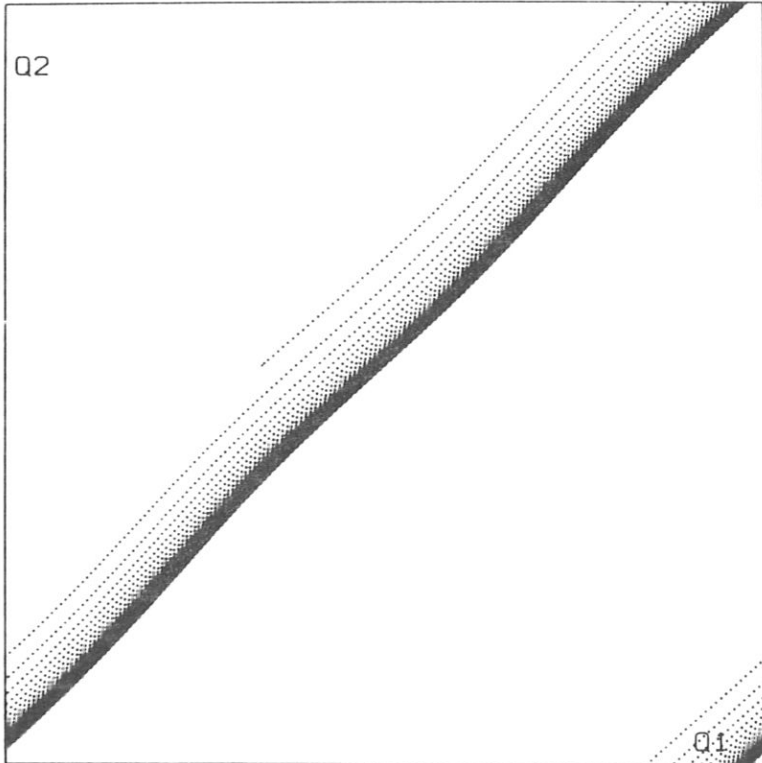


Fig. 4a

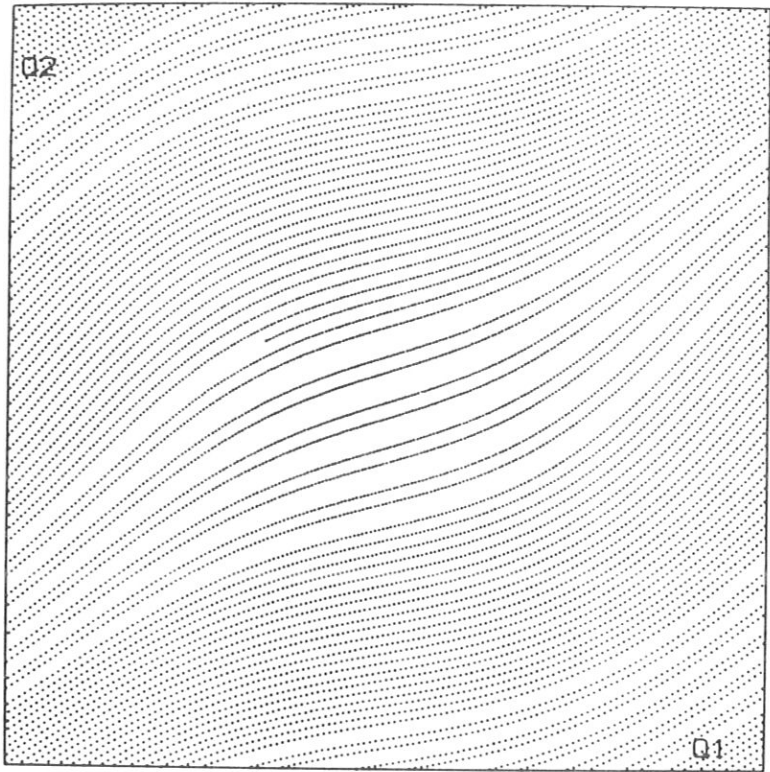
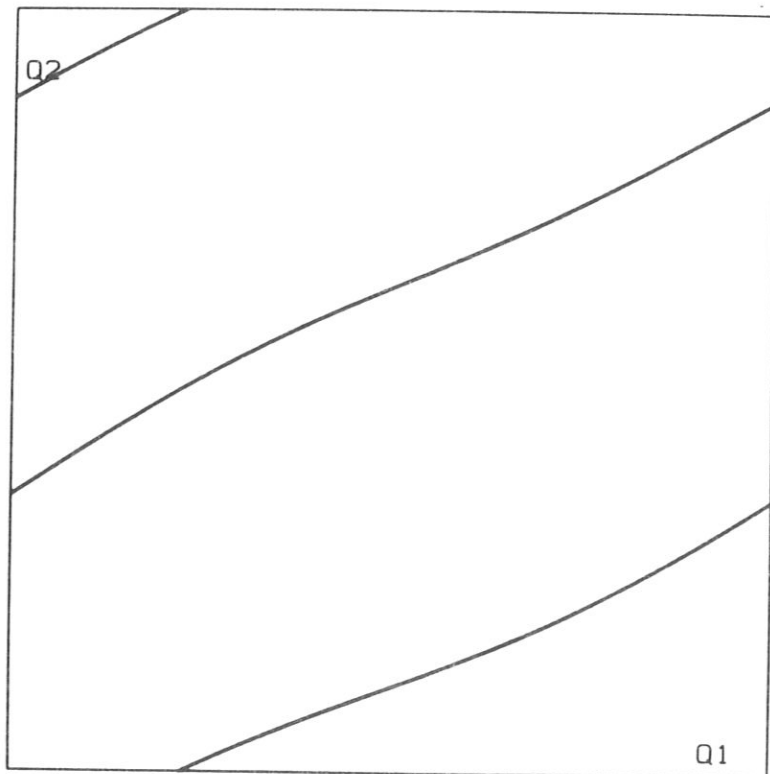


Fig. 4b



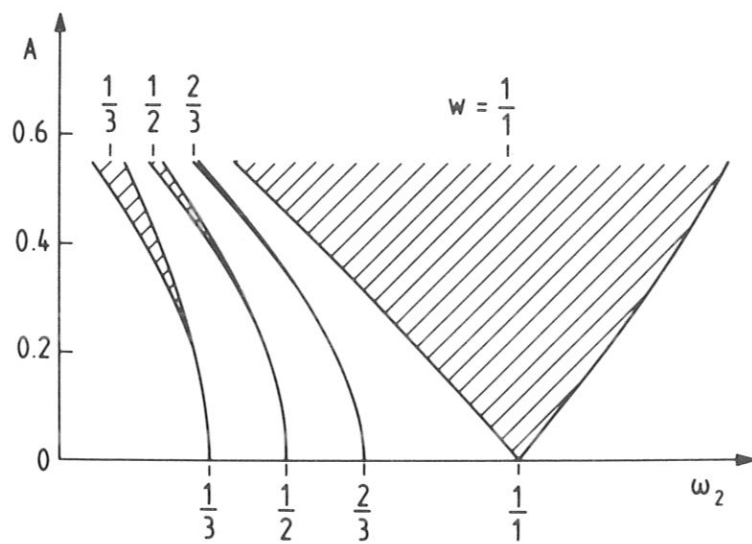


Fig. 5

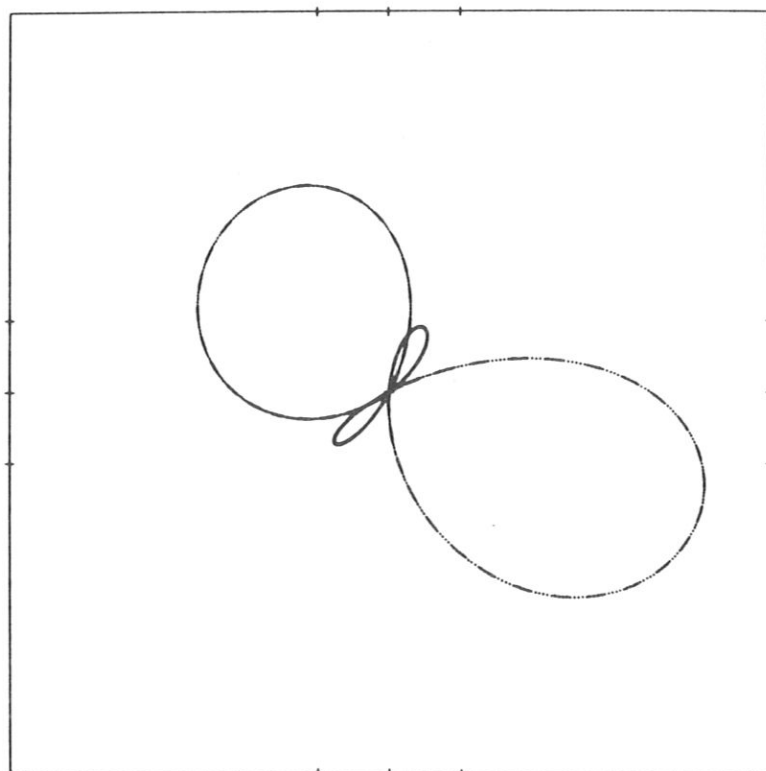


Fig. 6

Fig. 7a

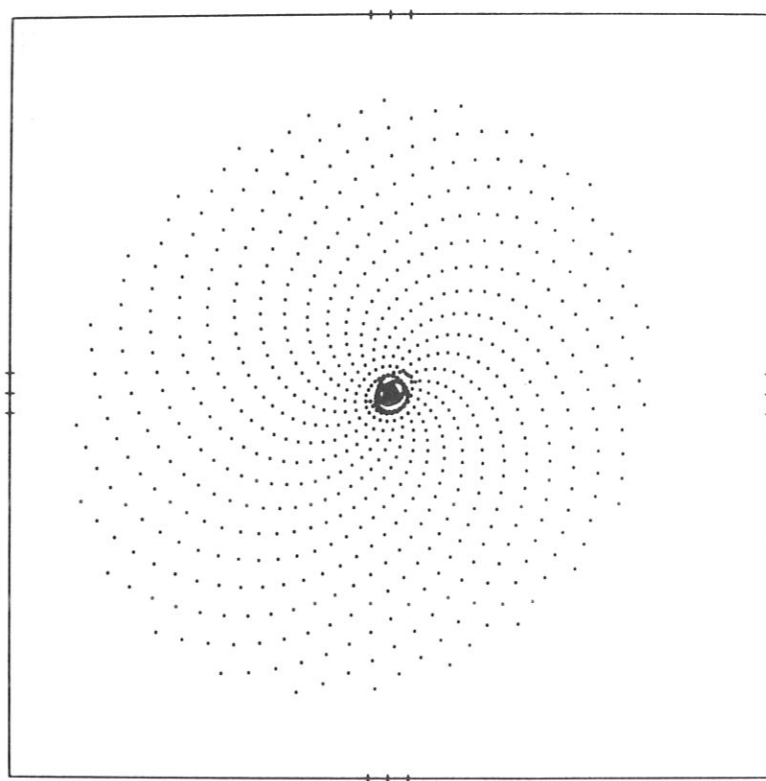


Fig. 7b

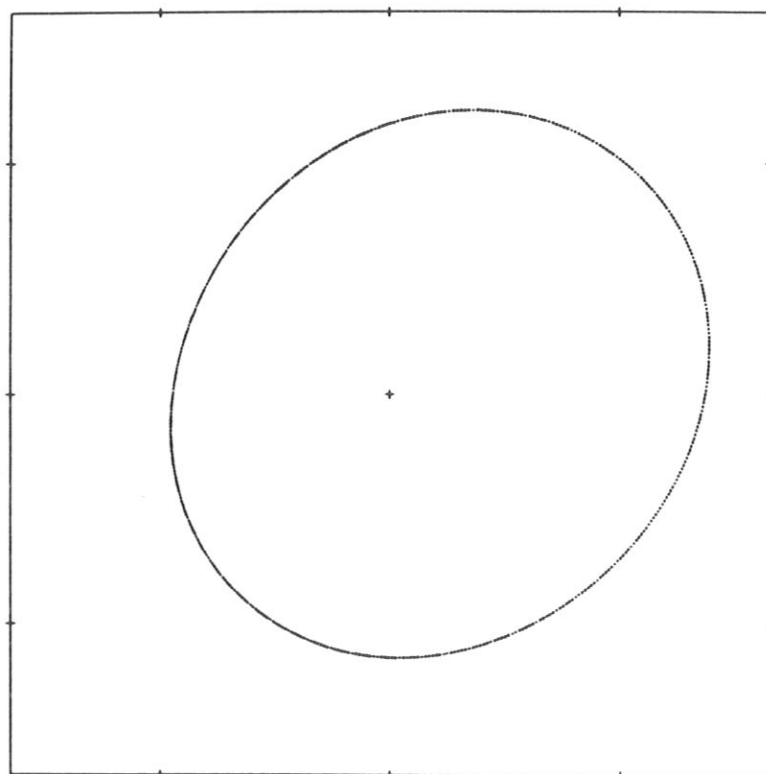




Fig. 8

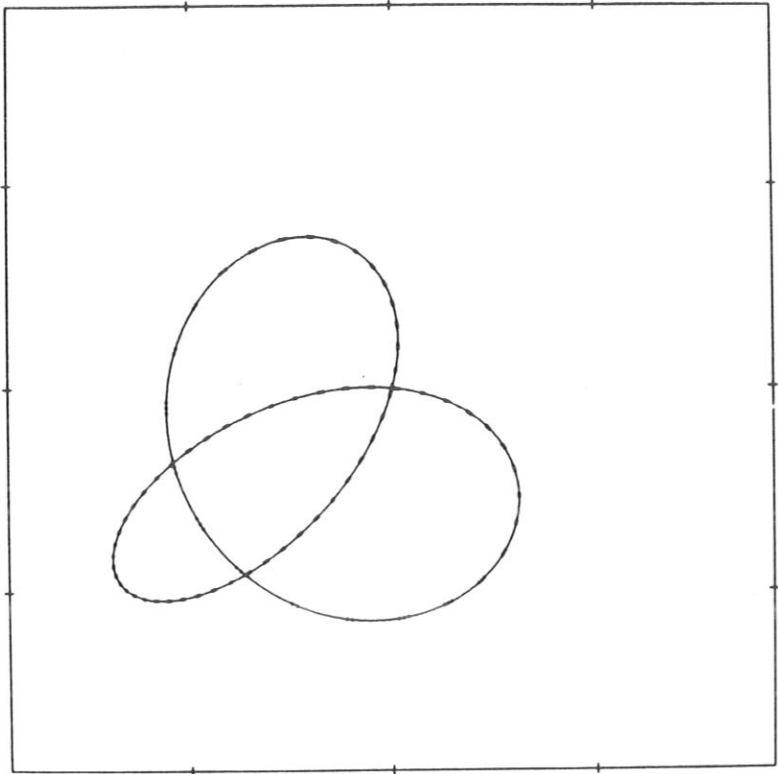


Fig. 9

